International Journal of Mechanical, Industrial and Aerospace Sciences
ISSN: 2517-9950
Vol:2, No:9, 2008

PID Parameter Optimization of an UAV Longitudinal Flight Control System

Kamran Turkoglu, Ugur Ozdemir, Melike Nikbay, and Elbrous M. Jafarov

***Abstract*—**In this paper, an automatic control system design based on Integral Squared Error (ISE) parameter optimization technique has been implemented on longitudinal flight dynamics of an UAV. It has been aimed to minimize the error function between the reference signal and the output of the plant. In the following parts, objective function has been defined with respect to error dynamics. An unconstrained optimization problem has been solved analytically by using necessary and sufficient conditions of optimality, optimum PID parameters have been obtained and implemented in control system dynamics.

***Keywords*—**Optimum Design, KKT Conditions, UAV, Longitudinal Flight Dynamics, ISE Parameter Optimization.

I. Introduction

IN recent years, development of feasible techniques for on-board mission management systems for Unmanned Aerial Vehicles (UAVs) has been seriously taken into account. From that point, existing UAV systems are generally guided remotely, which helps to control the flight trajectory of UAV by an integrated on-board auto pilot. Existing areas of use of UAVs are mainly concentrated on reconnaissance missions, observation, border security, combat missions etc. Moreover, there are some existing research projects dealing with a variety of possible applications of UAVs such as uninhabited combat aircraft, intervention rotorcraft, road traffic surveillance, pursuit, search and rescue helicopters, power cable inspection UAVs or forest fire surveillance aircraft [1]. During all of these missions UAVs are expected to be fault tolerant, to work in high precision, to be able to coordinate the coupling effects within the system dynamics and to have high maneuverability, and in order to be able to accomplish all of the desired performance characteristics, high fidelity in dynamic modeling should be achieved, where efficient control system design providing optimum performance limits should be accomplished.

In that sense, in this paper, an automatic control system design for longitudinal flight dynamics based on Integral Squared Error (ISE) parameter optimization technique has been implemented on UAV dynamics.

In literature, there are some existing studies on ISE parameter optimization technique such as establishing a hierarchy of dynamic accuracy with the ISE [2], constrained least square design of Finite Impulse Response (FIR) filters [3], decoupled method for approximation of signals by exponentials [4], an approach for handling the nonlinearities of High-Voltage-Direct-Current (HVDC) electric power transmission system for stability analysis [5], least squared error FIR filter design [6], optimal gain scheduling controller for a diesel engine [7], limitations on maximal tracking accuracy [8], mapping error of linear dynamic systems caused by reduced-order model [9]; besides, there are very limited amount of applications in literature related with ISE parametric optimization on aircrafts / UAVs. As a matter of fact, in many control applications in order to find an optimal solution for a given problem, optimal control theory is widely used, but in this case specifically parameter optimization is necessary and will be conducted through ISE parameter optimization technique.

In the first part of the paper, longitudinal dynamic modeling of an UAV will be presented. In the second part, mathematical background behind the ISE parameter optimization technique will be given. In the third section, closed-loop time domain results will be presented to complete the work.

II. Longitudinal Dynamics of an UAV

Before getting into the control system design, longitudinal flight characteristics should be analyzed. For this purpose, Equations of Motion (EoMs) governing the longitudinal flight, taken from [10], have been used for analysis as given in (1), where the first two are force equations in x and z directions, respectively, while M is the moment equation in y direction.

$$
\begin{aligned}
x:&\ (\frac{mu}{Sq}s - C_{X_u})'u(s) - C_{X_\alpha}'\alpha(s) - C_W(\cos\Theta)\theta(s) = 0 \\
z:&\ -C_{Z_U}'u(s) + \left[(\frac{mu}{Sq} - \frac{c.C_{Z\dot{\alpha}}}{2u})s - C_{z_\alpha}\right]'\alpha(s) \\
&+ \left[(-\frac{mu}{Sq} - \frac{c.C_{Zq}}{2u})s - C_W\sin\Theta\right]\theta(s) = 0 \\
M:&\ (-\frac{c.C_{m_{\dot{\alpha}}}}{2u}s - C_{M_\alpha})'\alpha(s) + (\frac{I_y}{Sqc}s^2 - \frac{c.C_{M_q}}{2u}s)\theta(s) = 0
\end{aligned}
\qquad (1)
$$

K. Turkoglu was with Istanbul Technical University, Istanbul, TURKEY. (Phone:1-646-301-6137; fax:1-612-626-1558; e-mail: kamran@aem.umn.edu)
U. Ozdemir is with Istanbul Technical University, Istanbul, TURKEY. (e-mail: ugur.ozdemir@itu.edu.tr).
M. Nikbay is with Istanbul Technical University, Istanbul, TURKEY. (e-mail: nikbay@itu.edu.tr).
E. M. Jafarov is with Istanbul Technical University, Istanbul, TURKEY. (e-mail: cafer@itu.edu.tr)..

where $'u$ = change of velocity in longitudinal flight, $'\alpha$ = change of angle of attack in longitudinal flight, Θ = pitch angle, θ = change of pitch angle from equilibrium point, so that $`u = u / U_0$ and $`\alpha = w / U_0$, where u is perturbation velocity in X direction, w is perturbation velocity in Z direction and U_0 is the steady state velocity in longitudinal flight. In addition, all capital C's with necessary subscripts represent corresponding stability derivatives, (Table II), of the UAV which are calculated with respect to the characteristic properties of UAV (Table I).

After the introduction of EoM, characteristic properties of UAV have been calculated in Table-1 and Table-2, respectively [11].

TABLE I
CHARACTERISTIC PROPERTIES OF UAV.

Symbol	Quantity	
m	mass	5 [kg]
U_0	steady state velocity	12 [m/sec]
g	gravitational force	9.807 [m/sec^2]
S	wing area	0.4205 [m^2]
$S_{vertical\ tail}$	vertical tail wing area	0.1323 [m^2]
ρ	air density	1.226 [kg/m^3]
I_{yy}	moment of inertia	0.1204 [m^4]
$L_{t/c}$	chord length	0.235 [m]

TABLE II
STABILITY DERIVATIVES AND INPUTS OF UAV.

Symbol / Quantity	Symbol / Quantity
C_{xu} = -0.0264	$C_{Za'}$ = -0.0347
C_{xa} = 1.2821	C_{Za} = -0.1381
C_D = 0.0132	C_{Zq} = -3.30
C_L = 1.3210	$C_{Ma'}$ = -0.0347
C_W = -1.3210	C_{Ma} = -0.0312
$L_{t/c}$ = 1	C_{Mq} = -3.30
C_{Zu} = -2.6424	$C_{X\delta e}$ = 0
$C_{Z\delta e}$ = -0.71	$C_{M\delta e}$ = -0.71

Since we are only interested in the change of pitch angle (θ) with respect to a given elevator deflection (δ_e) in longitudinal flight, only the θ/δ_e transfer function (TF) will be taken into consideration [10]. Using the characteristic properties and calculated stability derivatives, it is possible to construct the nominal plant TF of θ/δ_e as:

$$\frac{\theta(s)}{\delta_e(s)} = \left(\frac{1.423s^2 + 0.134s + 1.839}{0.02424s^4 + 0.06836s^3 + 0.1s^2 + 0.0859s + 0.0836} \right) \quad (2)$$

Also the corresponding modes in longitudinal flight and their characteristic properties could be simply derived from the denominator of (2), as shown in Table-3 [10].

TABLE III
CHARACTERISTIC PROPERTIES OF LONGITUDINAL FLIGHT.

Phugoid Mode	Short Period Mode
ξ_{pm} = 0.0147	ξ_{sm} = 0.517
ω_{pm} = 1.1152 rad/sec	ω_{sm} = 2.1152 rad/sec
T_{pm} = 61.1027 sec	T_{sm} = 0.9127 sec

As it is possible to see from both short period and phugoid mode, UAV is lightly damped (under-damped) in phugoid mode, while the damping ratio in short period mode is considerably good. After having an insight related with the open loop dynamics of the UAV, it is also possible to have a look at the frequency domain response of open loops dynamics. Therefore, Bode plot of TF has been plotted and is presented in Figure-1.

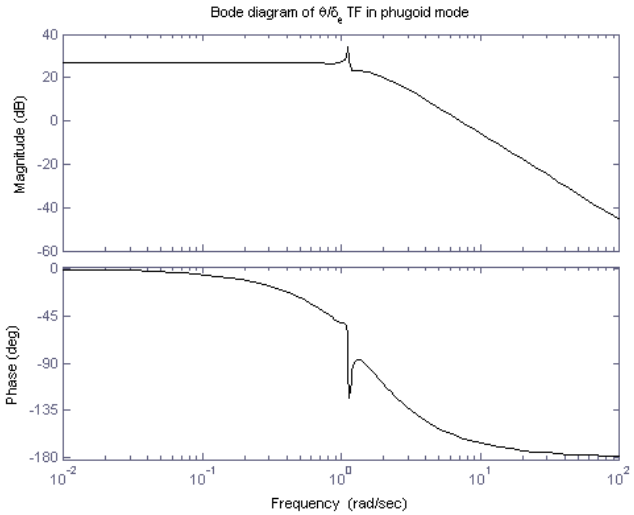

Fig.1 Frequency domain response of θ / δ_e TF.

As it is also possible to see from Fig.1, phugoid mode dynamics (ω_{n_pm} = 1.1152 rad/sec) are affected in a great manner for a given δ_e deflection. Furthermore, if the open loop time domain responses of θ / δ_e TF are plotted, it is probable to detect the responses as given in Fig.2, where Fig.2 represents the open loop (OL) time domain step response and the OL time domain impulse response, respectively.

III. CONTROLLABILITY

During PID parameter optimization process, which is going to be presented in the next section, control system design analysis will be implemented in system dynamics. And just before getting into the optimum design part, the controllability characteristic of the UAV system will be investigated.

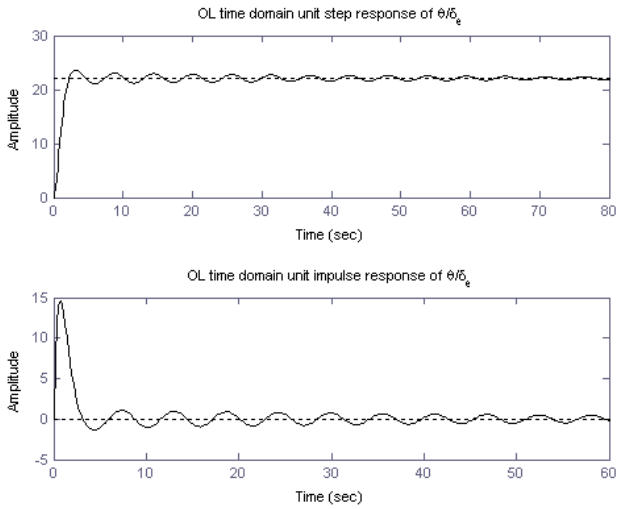

Fig.2 OL time domain responses of θ / δ_e TF.

It is known that the controllability matrix of a system, as defined in [12], is as

$$A_{nxn} \Rightarrow C_t = [B \quad AB \quad \dots \quad A^{n-1}B] \tag{3}$$

so that the controllability matrix must satisfy

$$Rank(C_t) = n \tag{4}$$

condition. In this way, the system is called reachable or controllable. If given controllability conditions are applied to given system dynamics, obtained results are as given in (5).

$$C_t = \begin{bmatrix} 1 & -2.4649 & 2.3250 & 0.4097 \\ 0 & 1 & -2.4649 & 2.3250 \\ 0 & 0 & 1 & -2.4649 \\ 0 & 0 & 0 & 1 \end{bmatrix} \Rightarrow Rank(C_t) = 4 = n \tag{5}$$

With such controllability analysis, it has been proved that the longitudinal UAV system is controllable, which enables the opportunity to implement the parameter optimized control system design method.

IV. Integral Squared Error Parameter Optimization

Optimization is a process which simply searches for any existing feasible and optimum solutions under specific circumstances. Here, the main goal is to minimize the performance index (PI), which is usually denoted by *J*, under the dynamical constraints of the physical system. In literature, numerous performance indices are defined for an optimal control system design. But in this paper, Integral Squared Error (ISE) parameter optimization method will be used.

As it is possible to see from Fig.3, in given control system design, there are three control parameters (K_i, T_i and T_d) to be optimized, which are *suggested* PID controller parameters.

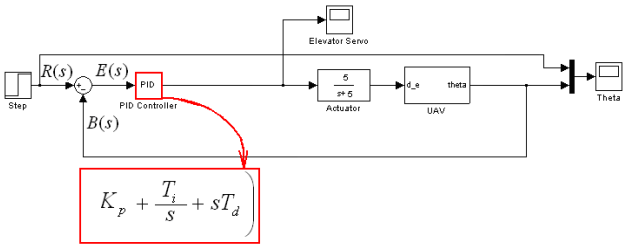

Fig.3 Simulink block diagram of optimal parameters system design.

Benefiting from [13-15], it is possible to characterize ISE parameter optimization method performance index as

$$(PI)_{ISE} = \int_0^\infty e^2(t)dt \tag{6}$$

where error function (*E(s)*) is commonly defined as

$$E(s) = \frac{R(s)}{1 + G(s)H(s)} \tag{7}$$

Here, *G(s)* is the TF of the nominal plant, *R(s)* is the (step) input TF and *H(s)* is the TF of the feedback line. According to these, for analysis, error function of the suggested optimized control system design has been derived from Fig.3 as

$$\begin{aligned} &E(s) = R(s) - B(s)\,,\; B(s) = G(s)PID(s)E(s) \\ &\Rightarrow E(s) = R(s) - G_{in}(s)PID(s)E(s) \\ &\frac{E(s)}{R(s)} = \frac{1}{1 + G(s)PID(s)}\,,\; PID(s) = K_p + \frac{T_i}{s} + sT_d \end{aligned} \tag{8}$$

where *G(s)* is the nominal plant (including the actuator dynamics), *PID(s)* is the transfer function of the PID controller. As it is likely to see from (8), given system dynamics is not extremely complicated and an explicit error function can be easily calculated. Steady state error incorporated performance indices are relatively easier to work with and they usually supply analytic solutions. Therefore, in order to make some simplifications in the performance index, in the following section Parseval's Theorem will be used.

A. Parseval's Theorem

Previously presented performance index, portrayed from [13-15], was defined as

$$J = \int_0^\infty f_1(t) f_2(t)\,dt \Rightarrow f_1(t) = f_2(t) = e(t) \Rightarrow J = \int_0^\infty e^2(t)\,dt \tag{9}$$

As it is likely to see from (9) performance index is evaluated in time (t) domain, but our error function (*E(s)*) was obtained in s-domain. Thus, if *J* could be expressed in terms of Laplace (s)-domain, then error function could be used for calculation purposes and will lead to great simplifications in the calculation. According to Parseval's theorem, integral given in (9) could be defined as

$$J = \frac{1}{2\pi i}\int_{-i\infty}^{+i\infty} F_1(s)F_2(s)ds \tag{10}$$

$$J = \int_0^{\infty} f^2(t)\,dt = \frac{1}{2\pi i}\int_{-i\infty}^{+i\infty} F(s)F(-s)ds\ ,\ f_1(t) = f_2(t) = f(t) \tag{11}$$

As it could be seen from (10) and (11), given integral provides the translation from time domain to s-domain. Generally, in linear dynamical systems F(s) is obtained as

$$F(s) = \frac{c(s)}{d(s)} = \frac{c_{n-1}s^{n-1} + c_{n-2}s^{n-2} + ... + c_1 s + c_0}{d_n s^n + d_{n-1}s^{n-1} + ...d_1 s + d_0} \tag{12}$$

where n is the degree of the system dynamics. Using (12) and (11), it is possible to obtain transfer function of system dynamics in integral form such as

$$J = \frac{1}{2\pi i}\int_{-i\infty}^{+i\infty} \frac{c(s)}{d(s)}\frac{c(-s)}{d(-s)}ds \tag{13}$$

where the value of the integral could be obtained in terms of c_i's and d_i's. In literature, there are several calculated integral tables which obtain a solution to the integral given in (13) and some of them are given for information in (14).

$$J_1 = \frac{{c_0}^2}{2d_0 d_1}$$

$$J_2 = \frac{{c_1}^2 d_0 + {c_0}^2 d_2}{2d_0 d_1 d_2}$$

$$J_3 = \frac{{c_2}^2 d_0 d_1 + ({c_1}^2 - 2c_0 c_2)d_0 d_3 + {c_0}^2 d_2 d_3}{2d_0 d_3(-d_0 d_3 + d_1 d_2)} \tag{14}$$

$$J_4 = \frac{\left\{ {c_1}^2(-{d_0}^2 d_3 + d_0 d_1 d_2) + ({c_2}^2 - 2c_1 c_3)d_0 d_1 d_4 + \right\}}{\left\{ ({c_1}^2 - 2c_0 c_2)d_0 d_3 d_4 + {c_0}^2(-{d_4}^2 d_1 + d_2 d_3 d_4) \right\}} \Big/ 2d_0 d_4(-d_0 {d_3}^2 - d_4 {d_1}^2 + d_1 d_2 d_3)$$

B. PID Parameter Optimization

As it could be seen from Fig.3, in the control system block diagram, we have three PID controller gains which are K_p, T_i and T_d. In order to find the optimal values of gains, ISE parameter optimization method will be applied as follows.

A generic optimization problem associated with a given system can be formulated as

$$\begin{aligned} &\min_{x\in X}\ z(x) \\ &h(x) = 0\ ,\ h(x) \in R^{n_h} \\ &g(x) \le 0\ ,\ g(x) \in R^{n_g} \\ &X = \{x \in R^{n_s} \mid x_L < x < x_u\} \end{aligned} \tag{15a}$$

where x is a set of n_x abstract parameters restricted by lower and upper bounds x_L and x_U, z is a cost function of interest, h denotes a set of n_h equality constraints, g is a set of n_g inequality constraints.

A constrained optimization problem can be transformed to an unconstrained optimization problem by using the Lagrange multiplier method as follows

$$L(x_i, \eta_i, \gamma_i) = \underbrace{z(x_i)}_{\substack{objective \\ function}} + \underbrace{\sum_0^{n_h} \eta_i h_j(x_i)}_{\substack{equality \\ constra\,int\,s}} + \underbrace{\sum_0^{n_h} \gamma_i g_j(x_i)}_{\substack{inequality \\ constra\,int\,s}} \tag{15b}$$

where L is Lagrange function, η_i and γ_i are Lagrange multipliers [16]. The optimum of a constrained optimization problem is characterized by the saddle point of the Lagrange function in the primal and dual solution space. Thus

1) $\min_x L(x,\eta,\gamma)$ in the primal space
2) $\max_x L(x,\eta,\gamma)$ in the dual space

The saddle point of the Lagrange function is governed by the Karush-Kuhn-Tucker (KKT) necessary conditions. This condition ensured that optimum point lies on tangent planes with respect to all primal and dual variables. Therefore

$$\begin{aligned} &\nabla L = \frac{\partial L}{\partial x_j} + \frac{\partial L}{\partial \eta_j} + \frac{\partial L}{\partial \gamma_j} = 0 \quad \text{where} \\ &\frac{\partial L}{\partial x_j} = 0 \quad \text{holds for} \quad \nabla z + \sum_j^{n_h} \eta_j \nabla h_j + \sum_j^{n_g} \gamma_j \nabla g_j = 0 \\ &\frac{\partial L}{\partial \eta_j} = 0 \quad \text{holds for} \quad h_j = 0 \\ &\frac{\partial L}{\partial \gamma_j} = 0 \quad \text{holds for} \quad \gamma_j g_j = 0 \ \text{ and } \ \gamma_j \ge 0 \end{aligned} \tag{16}$$

KKT conditions are necessary but not sufficient for a saddle point. Additionally, we need that the Lagrange function is convex with respect to the optimization variables in the primal solution space which is the sufficient condition for optimality.

According to given UAV dynamics (θ / δ_e), given problem is an unconstrained optimization problem. Objective function that is going to be minimized in this study is the error function, $E(s)$, and corresponding optimization variables are K_p, T_i and T_d. Consequently, the optimization procedure can be summarized as :

i. Obtain the corresponding error function (8) from the suggested block diagram (Fig.3)
ii. Obtain the performance index representation in terms of c_i's and d_i's.
iii. Calculate the optimum solution by applying the KKT conditions ($\partial J_n / \partial x = 0$) and verify the convexity (Hessian) of the point ($\partial^2 J_n / \partial x^2 > 0$)

First of all, the error function should be obtained for minimization purposes. Previously a general form of error function $E(s)$ has been obtained in (8) which leads to

$$\frac{E(s)}{R(s)} = \frac{\left((s+5)(s^2+1.03156\,s+2.99349)\right)}{\left\{\begin{array}{l} s^4+\left(6.03156+4.2793\,T_d\right)s^3 \\ +\left(8.15129+4.2793\,K_p+10.1351T_d\right)s^2 \\ +\left(14.9675+10.1351K_p+4.2793T_i\right)s+10.1351T \end{array}\right\}} \quad (17)$$

for given UAV dynamics. It is possible to see that the order of the system is $n = 4$ and therefore J_n, which corresponds to J_4, needs to be calculated. In this case, coefficients of the integral becomes: $c_0 = 14.9675$, $c_1 = 8.15129$, $c_2 = 6.03156$, $c_3 = 1$, $c_4 = 0$, $d_0 = 10.1351*T_i$, $d_1 = 14.9675 + 10.1351*K_p + 4.27932*T_i$, $d_2 = 8.15129 + 4.27932*K_p + 10.1351*T_d$, $d_3 = 6.03156 + 4.27932*T_d$ and $d_4 = 1$.

Since we obtained necessary c_i's and d_i's, we are able to evaluate J_4 as

$$J_4 = \frac{\left\{\begin{array}{l} 377.951+479.338\,T_d^2-180.174\,T_i+21.6856\,K_p^2\,T_i \\ +29.8342\,T_i^2+T_d\,(1061.13-168.31T_i)+K_p\,\{9.1563 \\ (1.04691+T_i)(18.0737+T_i)+T_d\,(202.391+51.3597\,T_i)\} \end{array}\right\}}{\left\{\begin{array}{l} T_i\,\{K_p^2\,(158.876+185.599T_d)+T_d\,(1437.06-112.324T_i) \\ +649.156T_d^2-18.3126(-1.6194+T_i)\,(17.2599+T_i) \\ +Kp[581.223+439.569T_d^2+23.7112T_i+T_d\,(1247.18 \\ +78.3655T_i)]\} \end{array}\right\}} \quad (18)$$

After deriving the objective function. J_4, using KKT and convexity conditions, it is possible to find optimum design parameters of the desired control system by solving equations given in (16), simultaneously as follows

$$\min_{x\in X}(J_4) \quad \text{where } X=\{x\in R^3 \mid x_L < x < x_U\} \quad (19)$$

Since the problem is an unconstrained optimization problem, KKT necessary conditions reduce to

$$\frac{\partial J_4}{\partial K_p}=0 \quad , \quad \frac{\partial J_4}{\partial T_d}=0 \quad \text{and} \quad \frac{\partial J_4}{\partial T_i}=0 \quad (20)$$

By solving (20) it is possible to obtain optimum PID parameters as $K_p^* = 1.155415$, $T_i^* = 1.954899$, $T_d^* = 0.728157$ and if the necessary conditions are verified, they are obtained as follows

$$\begin{array}{l} \nabla_{K_p} J_4 = 0.0606\ 10^{-8} \cong 0\,,\ \nabla_{T_i} J_4 = 0.0904\ 10^{-8} \cong 0 \\ \nabla_{T_d} J_4 = 0.0924\ 10^{-8} \cong 0 \end{array} \quad (21)$$

If the sufficient condition of optimality-(Hessian) of the given solution parameters is checked, obtained results are as follows

$$\begin{array}{l} \nabla^2_{K_p} J_4 = 0.054591 > 0\,,\ \nabla^2_{T_i} J_4 = 0.114831 > 0 \\ \nabla^2_{T_d} J_4 = 0.210070 > 0 \end{array} \quad (22)$$

where it is possible to see that both necessary–sufficient optimality conditions are satisfied, which leads us to optimum parameters.

Using calculated (K_p^*, T_i^* and T_d^*) optimal parameters, time domain results of longitudinal flight control system are obtained as shown in Fig.4.

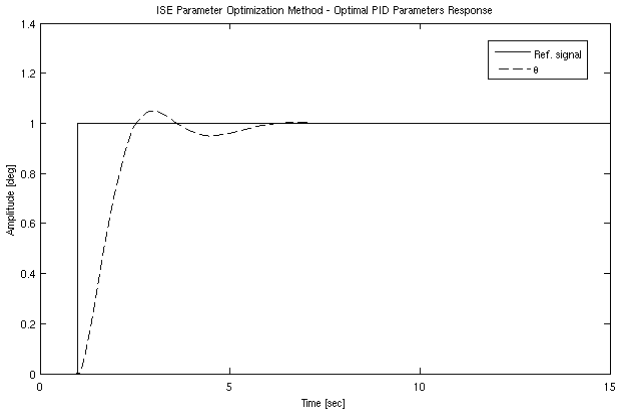

Fig.4 Time domain results of optimized PID controlled UAV system.

As it is possible to see from Fig.4, the settling time is nearly 5.5 seconds, which is a considerable value and the maximum control effort reached is 1 Newton. Maximum overshoot is only 5%, which is also remarkable.

V. Conclusion

In this paper, an optimized control system design based on Integral Squarred Error parameter optimization method has been aimed. In the first part of the paper, longitudinal dynamic modeling has been given and open loop time domain responses have been investigated. Objective function has been obtained, next KKT necessary and convexity sufficient optimality conditions have been applied into the system dynamics. Obtained optimal parameters have been used to obtain the closed time domain results. It has been observed that, optimal parameters are able to shape system dynamics relatively good so that the settling time is nearly 5.5 seconds and the maximum control effort is 1 Newton, while the maximum overshoot is only 5%.

References

[1] P. Fabiani, V. Fuertes, A. Piquereau, R. Mampey and F. Teichteil-Konigsbuch, "Autonomous flight and navigation of VTOL UAVs: from autonomy demonstrations to out-of-sight flights" in *Aerospace Science and Technology*, Vol. 11, Issues 2-3, p:183-193, March-April 2007

[2] E. Layer, "Theoretical principles for establishing a hierarchy of dynamic accuracy with the integral-square-error as an example" *IEEE Transactions in Instrumentation and Measurement* , Volume 46, Issue 5, Oct. 1997 pp:1178 – 1182

[3] I.W. Selesnick, M. Lang, C.S. Burrus, "Constrained least square design of FIR filters without specified transition bands" in *IEEE Transactions on Signal Processing*, Volume 44, Issue 8, Aug. 1996 pp:1879 – 1892.

[4] J. Lin and J. G. Proakis, "An enhanced optimal windowed RLS algorithm for fading multipath channel estimation" *in MILCOM '93. `Communications on the Move'.* Conference Record (Cat. No.93CH3260-7), 1993, p 1003-7 vol.3.

[5] P.K. Kalra, "An approach for handling the nonlinearities of HVDC system for stability analysis" *in IEEE Transactions on Power Electronics, v 5, n 3, July 1990, p 371-7.*

[6] C. S. Burrus, A. W. Soewito and R. A. Gopinath, "Least squared error FIR filter design with transition bands" *in IEEE Transactions on Signal Processing*, v 40, n 6, June 1992, p 1327-40.
[7] J. Jiang, "Optimal gain scheduling controller for a diesel engine" *in IEEE Control Systems Magazine, v 14, n 4, Aug. 1994, p 42-8*.
[8] C. Jie, Q. Li and O. Toker, "Limitations on maximal tracking accuracy" *in IEEE Transactions on Automatic Control, v 45, n 2, Feb. 2000, p 326-31*.
[9] E. Layer, "Mapping error of linear dynamic systems caused by reduced-order model" *in IEEE Transactions on Instrumentation and Measurement, v 50, n 3, June 2001, p 792-800*.
[10] J. H. Blakelock, Automatic Control of Aircrafts and Missiles, Wiley, 1991.
[11] K. Turkoglu, Investigation the Modes of Hezarfen UAV and Automatic Control Systems' Design, *BSc Thesis*, Istanbul Technical University, Istanbul, Turkey. 2007.
[12] K. Ogata, Modern Control Engineering, Addison Wesley, 1992.
[13] Gradshteyn, I. S. and Ryzhik, I. M. *Tables of Integrals, Series, and Products*, 6th ed. San Diego, CA: Academic Press, p. 1101, 2000.
[14] Kaplan, W. *Advanced Calculus, 4th ed.* Reading, MA: Addison-Wesley, p. 501, 1992.
[15] D. E. Kirk, *Optimal Control Theory : An Introduction*, 2nd editions, Dover Publications, 2007.
[16] J. S. Arora, *Introduction to Optimum Design,* Academic Press; 2nd edition (May 19, 2004).